VTT Technical Research Centre of Finland

Project report: Behaviour of Copper under Load Transients

Rantala, Juhani; Pohja, Rami

Published: 28/02/2023

Document Version
Publisher's final version

RESEARCH REPORT

VTT-R-00131-23

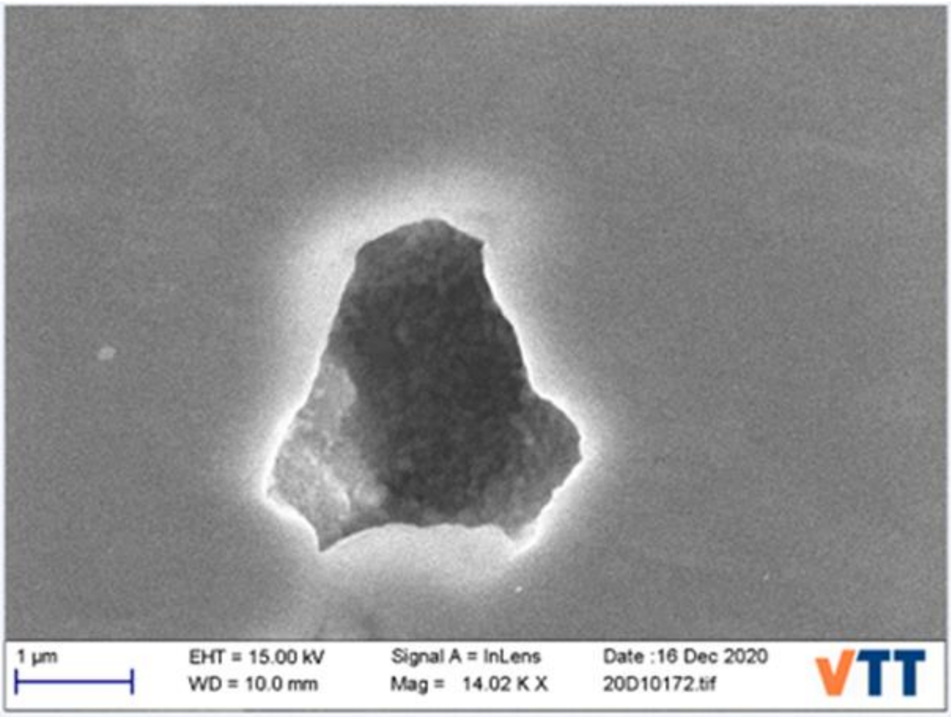

Project report: Behaviour of Copper under Load Transients

Authors: Juhani H. Rantala, Rami Pohja

Confidentiality: VTT Public

beyond the obvious

Report's title		
Project report: Behaviour of Copper under Load Transients		
Customer, contact person, address		**Order reference**
Nuclear Waste Management Fund		
Project name		**Project number/Short name**
BECOLT Behaviour of Copper under Load Transients		BECOLT
Author(s)		**Pages**
Juhani H. Rantala, Rami Pohja		21
Keywords		**Report identification code**
Cu-OFP, Nuclear waste disposal, copper canister, creep, relaxation		VTT-R-00131-23

Summary

This report summarises the main results of the BECOLT project which was running in 2019-2022 under the KYT2022 framework programme [1] funded by the National Nuclear Waste Management Fund (VYR). This project is continuation of the previous four-year project "Experimentally verified model-based predictions for integrity of copper overpack", PRECO under the KYT2018 framework programme.

Confidentiality	VTT Public

Espoo 28.2.2023

Written by	**Reviewed by**
J.H. Rantala	Rami Pohja
Senior Researcher	Senior Researcher

VTT's contact address
VTT, P. O. Box 1000, FI-02044 VTT, Finland. Tel. + 358 20 722 111 (exchange).
email: firstname.surname@vtt.fi

Distribution (customer and VTT)

KYT, 1 copy
VTT, 1 copy

Contents

1. Introduction

In the repository for spent fuel, the temperature of the canister surface is expected to peak at about 75-90°C before the first hundred years [2], with gradual cooling to the level of the bedrock environment (Figure 1). If a decision is to place the canisters closer to each other, the temperature will increase. The top temperature will depend also on the rate of wetting in individual disposal holes, which might vary a lot, depending on the flow of water in the bedrock. Therefore, it is possible, that at least some canisters will experience peak temperatures of 90°C and above. The development of the swelling pressure in bentonite surrounding the canisters will also depend on the rate of wetting.

For the protective copper (Cu-OFP) overpack of the canister, creep and corrosion are included as potential damage mechanisms under the repository conditions [2]. Although relatively mild in usual engineering terms, the repository conditions imply a technical challenge to life estimation for ensuring the integrity of the overpack. This is because of the discrepancy between the longest achievable laboratory tests (decades) compared to the design life that is of the order of glaciation cycles (about 10^5 years) to reduce the radioactivity of the contents close to the background level. The time difference by a factor of almost 10^4 also exceeds the usual range of extrapolation from laboratory experiments to real service conditions in most (or any) comparable engineering applications.

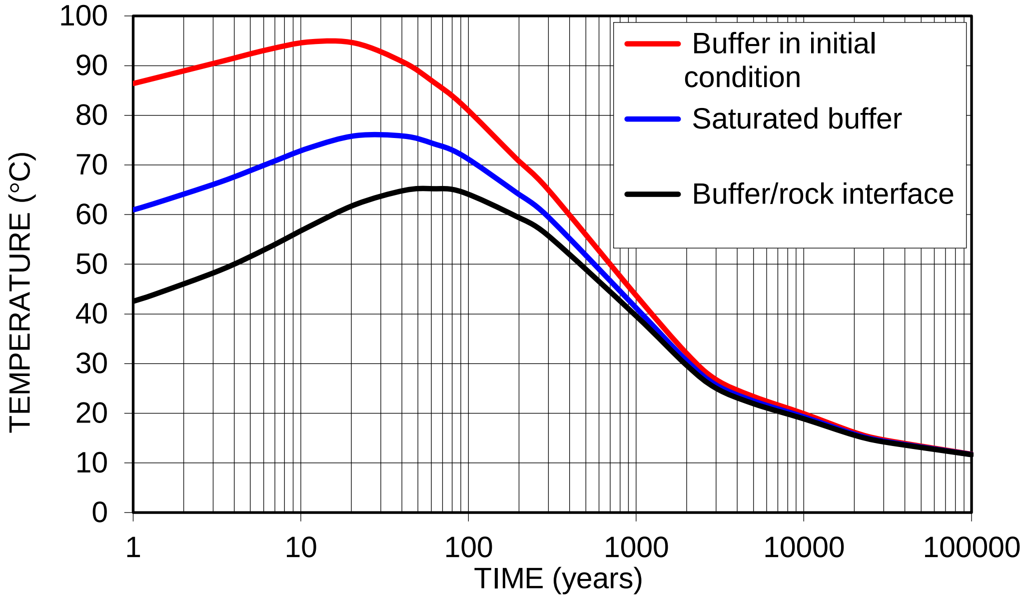

Figure 1. Predicted temperature evolution at the canister surface for EPR fuel [2]; the red curve assumes dry environment with a 10 mm gap around the canister.

2. Goal

At the beginning of the four-year period the following five themes were selected for the project:

1. OFP Copper has shown unexpected behaviour under certain loading conditions like unloading+re-loading and stepwise loading, which are relevant in the transient phase of the repository and especially during uneven swelling of the bentonite. The current creep models cannot explain these phenomena.
2. The effect of copper grain size is not well characterised and only few test results are available. The grain size will become large is certain areas of the canister and the large grain size will reduce the ductility of copper, possibly leading to fracture.
3. Relaxation behaviour of copper has been addressed in previous programme, but the current relaxation model is based on insufficient data base.
4. The combined effect of creep and corrosion is saline ground water has been studied before, but the corrosion reactions in those tests were most likely due to galvanic corrosion between the test specimen and the loading arrangement.
5. The early stages of damage behaviour of copper are not well understood and need to be investigated.

3. Long-term uniaxial testing

During the project two long-term uniaxial creep tests for Cu-OFP were running:

1) y211 V1 at 120MPa 152ºC

2) y303 K3 at 70MPa 200ºC

These specimens were extracted from the OFP copper canister tube T31 delivered by SSM/SKI (Sweden). The strain versus time curve is shown in Figure 2. The test y211 was interrupted for inspection at 170849 hours (19.5 years) at a strain of 32.3% and has been continued. The strain rate curve is shown in Figure 3 which indicates that the test is has reached the minimum strain rate. Figure 4 shows that the test y211 has already passed the expected rupture life predicted by the Wilshire equation [3] where the creep stress is normalised by the ultimate tensile strength at the creep testing temperature. During the four interruptions the gauge diameter has been measured and the results are shown in Figure 5. Oxide cracking has been observed during the inspections and it seems that the length of the cracks has not grown but the number of cracks is increasing with time. The depth of the cracks cannot be measured without cutting the specimen, but it is assumed that the cracks are in the oxide. This single test result is valuable in the sense that it shows that creep ductility of Cu-OFP remains high to long times with a strain of over 32% at the time of minimum strain rate. If we assume that the minimum creep rate is achieved at about mid-life of the test, then the rupture time of this test will become about 40 years.

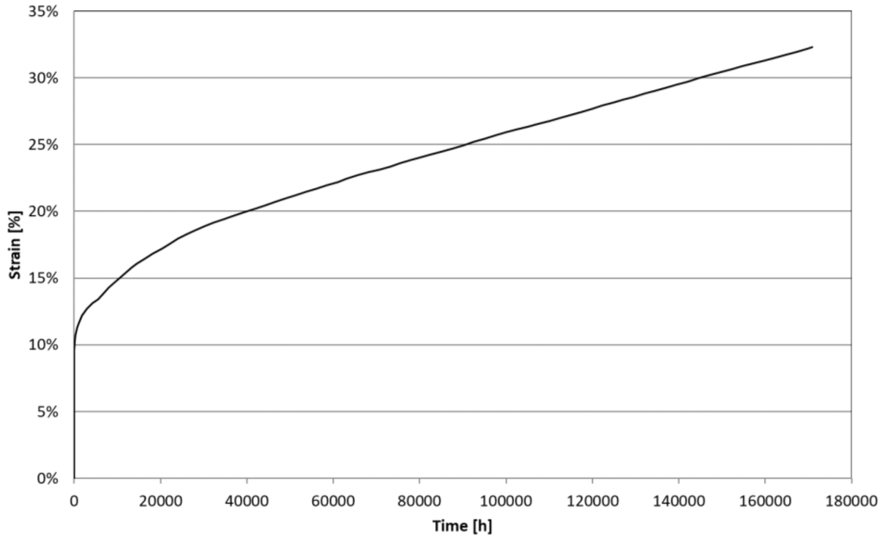

Figure 2. Strain vs. time curve of the test y211 at 120MPa 152ºC after 170849 hours.

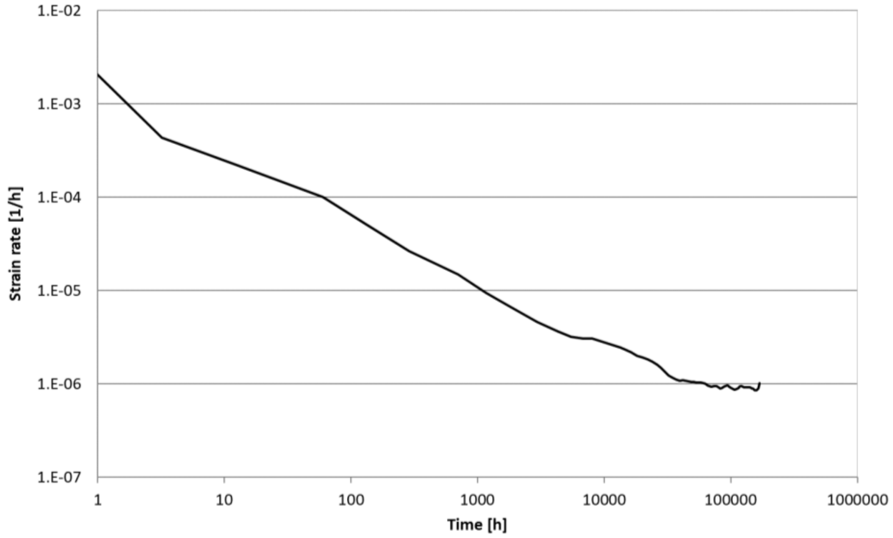

Figure 3. Strain rate curve of the test y211 at 120MPa 152ºC after 170849 hours.

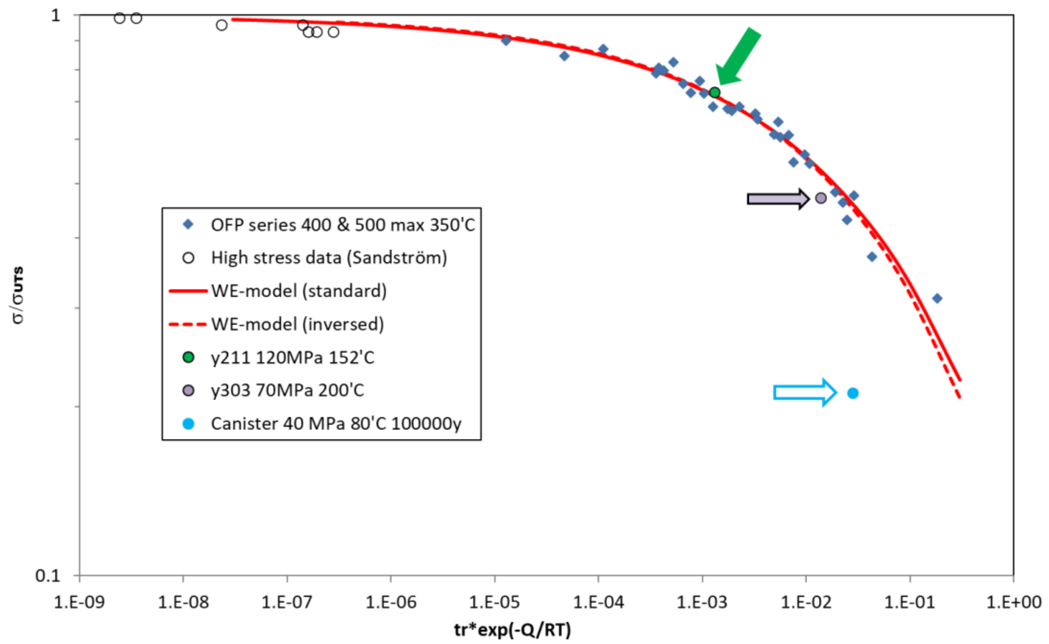

Figure 4. Wilshire plot for Cu-OFP

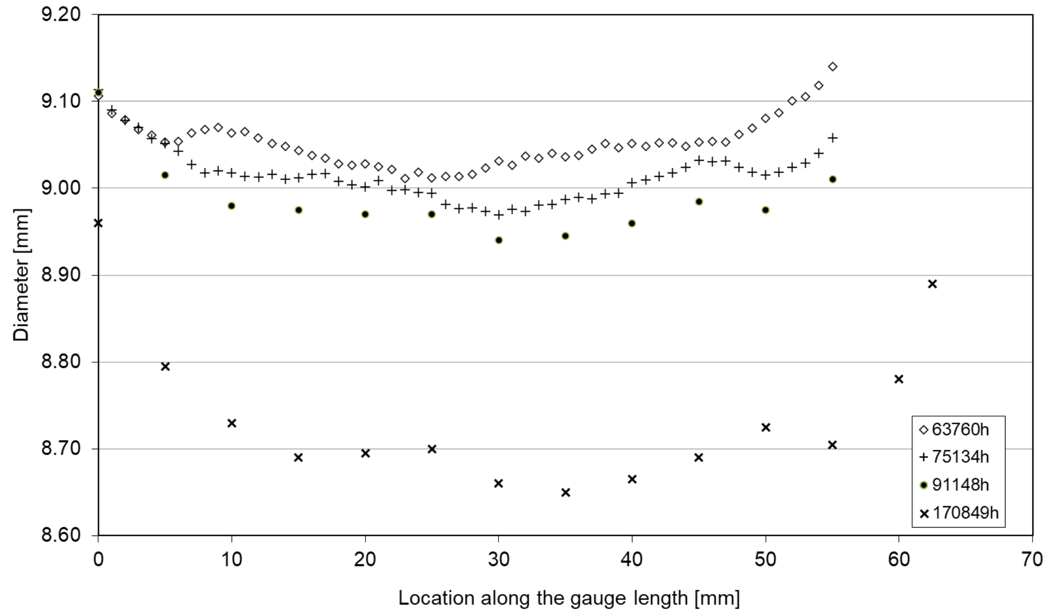

Figure 5. The gauge diameter measurements of the test y211 at four interruptions. Original gauge diameter has been 10.00 mm.

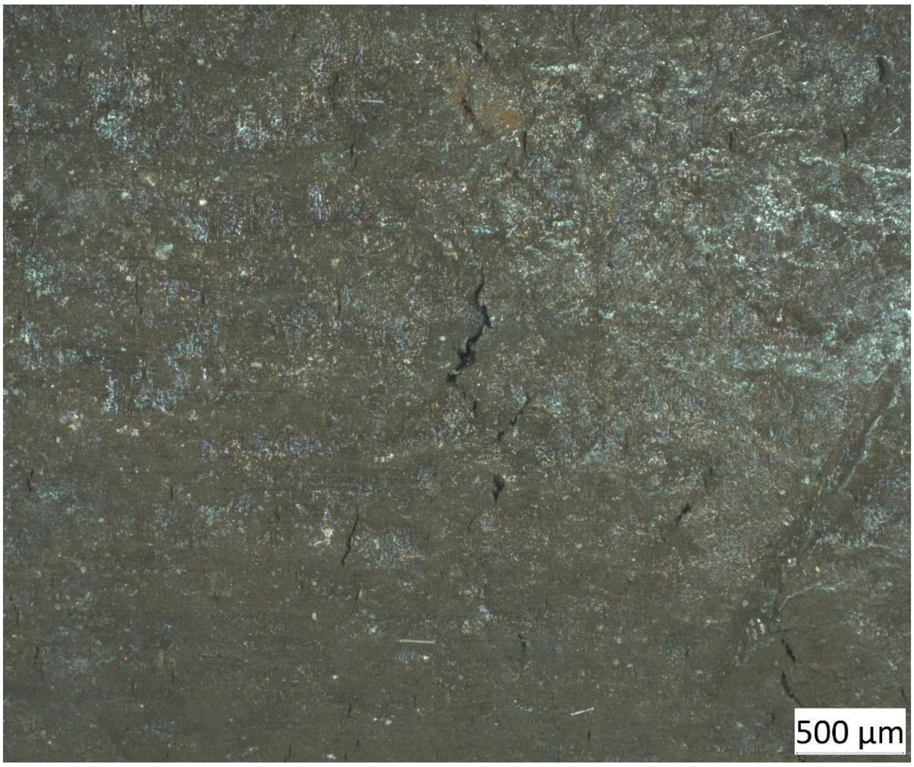

Figure 6. Oxide cracks in the specimen y211 after 170849 hours.

The test y303 at 70MPa 200ºC was terminated after 117523 hours (13.4 years) at 10.0% strain. The strain and strain rate curves are shown in Figure 7 and Figure 8 respectively. Although the strain rate had already started to turn towards the minimum strain rate it was estimated that the test would become too long to be continued to rupture because the strain was currently only 10.0%, so the test was terminated permanently. As can be seen from Figure 4, the testing time is still far from the predicted rupture time in the Wilshire plot. In the same graph the canister lifetime of 100000 years is shown at a postulated average stress and temperature of 40MPa at 80ºC. The specimen can be used in the future projects for inspection of early creep damage.

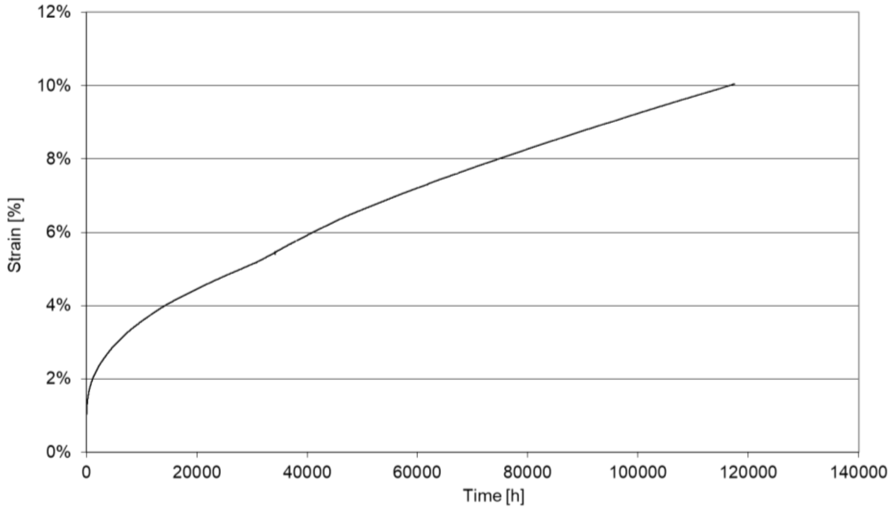

Figure 7. Strain vs. time of the test y303 at 70MPa 200ºC.

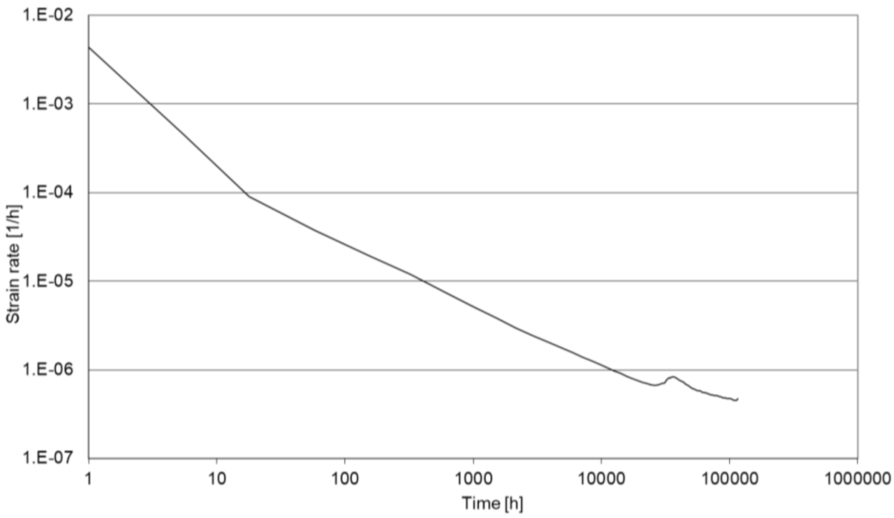

Figure 8. Strain rate vs. time of the test y303 at 70MPa 200ºC.

4. Load history dependence

A strong load history dependence in the creep behaviour of Cu-OFP was first reported by SKB [4]. The load was applied at 75ºC in a stepwise manner by first applying only 80% of the load for a fixed period, after which the load was increased to 90% and held for the same period and finally the full load was applied. As shown in Figure 9, the effect of this type of loading was that the rupture time decreased strongly, which is surprising and looks contradictory because the test is eased in the beginning, and one would expect the total testing time to become longer.

The main testing temperature of SKB has been 75ºC, so in the KYT project VTT wanted to find out whether a similar load history dependence would appear at the main testing temperature of 175ºC of the Finnish programme. Therefore, the load was applied in a similar way from 80% to 90% and to 100% of 135MPa and by using waiting periods of 2, 1 and 0.5 weeks between load changes as shown in Figure 10. When the rupture time of the continuous test y553 was 3087 hours the rupture time with 2 week waiting period was 1964 hours. The shorted rupture time of 1207 hours with one week waiting period.

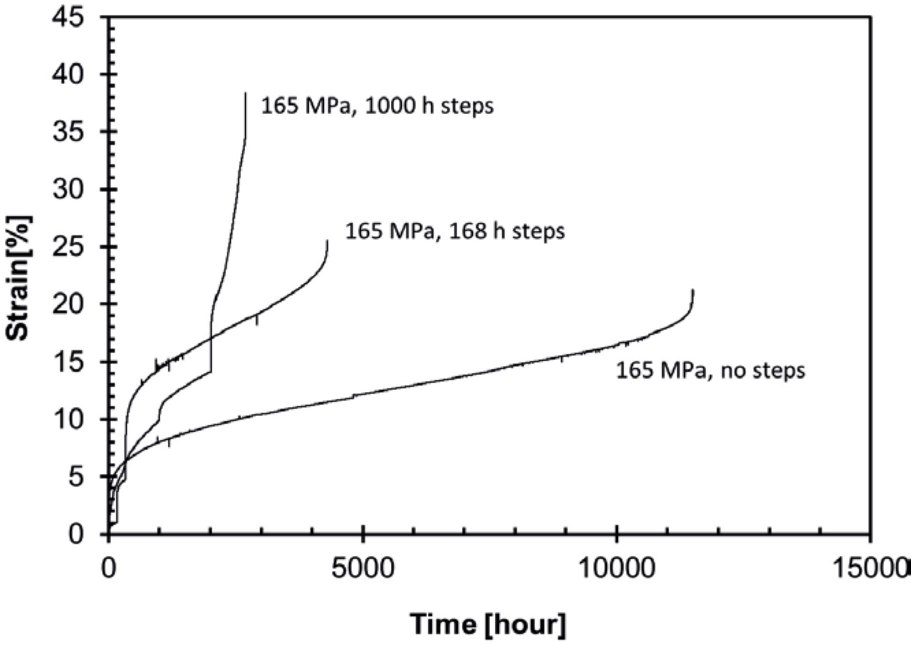

Figure 9. The effect of step-loading at 75ºC by SKB [4].

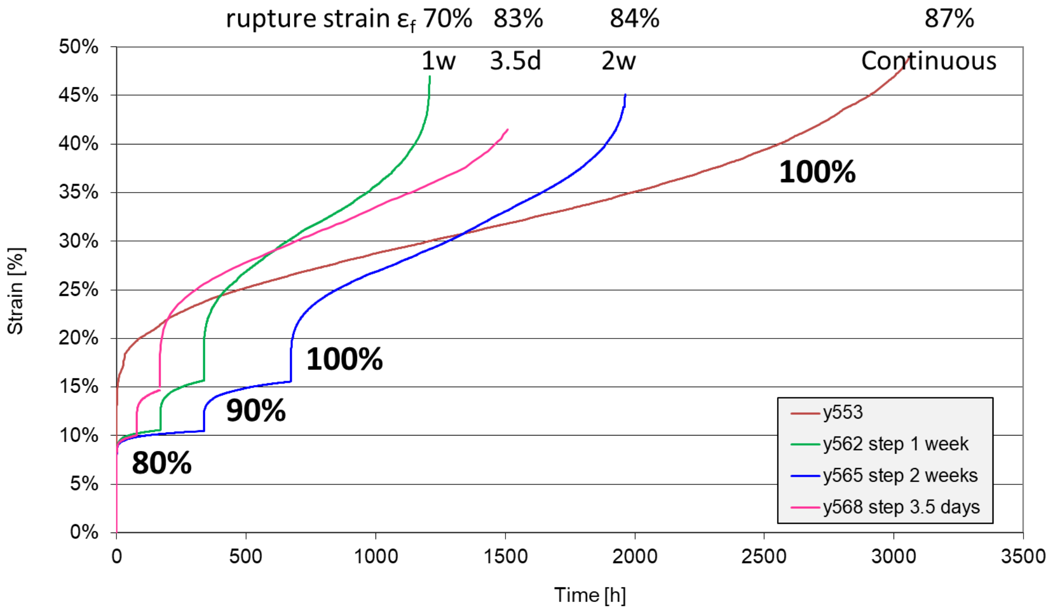

Figure 10. Effect of stepwise loading at 175ºC and full load of 135MPa.

As the main testing temperature of 75ºC does not represent the actual peak temperature, which the canister is going to experience during the first tens of years in the repository but is some kind of average temperature over the "hot period" of the repository, VTT wanted to perform a similar test series at 165MPa full load and 90ºC, which is the likely peak temperature the canister wall will experience. The waiting periods of 1,2 4 and 8 weeks were applied and load steps of 80, 90 and 100%. The strain curves are shown in Figure 11. The continuous test y563 was interrupted at 25540 hours at 38.1% strain after well passing the minimum creep rate of 4.24E-6 1/h. For the creep curves at 100% load and 2-8 week waiting period the continuous creep curve is shifted horizontally so that the curve coincides with the beginning of each of the 100% load steps. It can be seen that the preceding load steps have not had any remarkable acceleration of strain. It is surprising that the stepwise loading had a strong effect at 75ºC (tested by SKB) and at 175ºC (tested by VTT), but not at 90ºC.

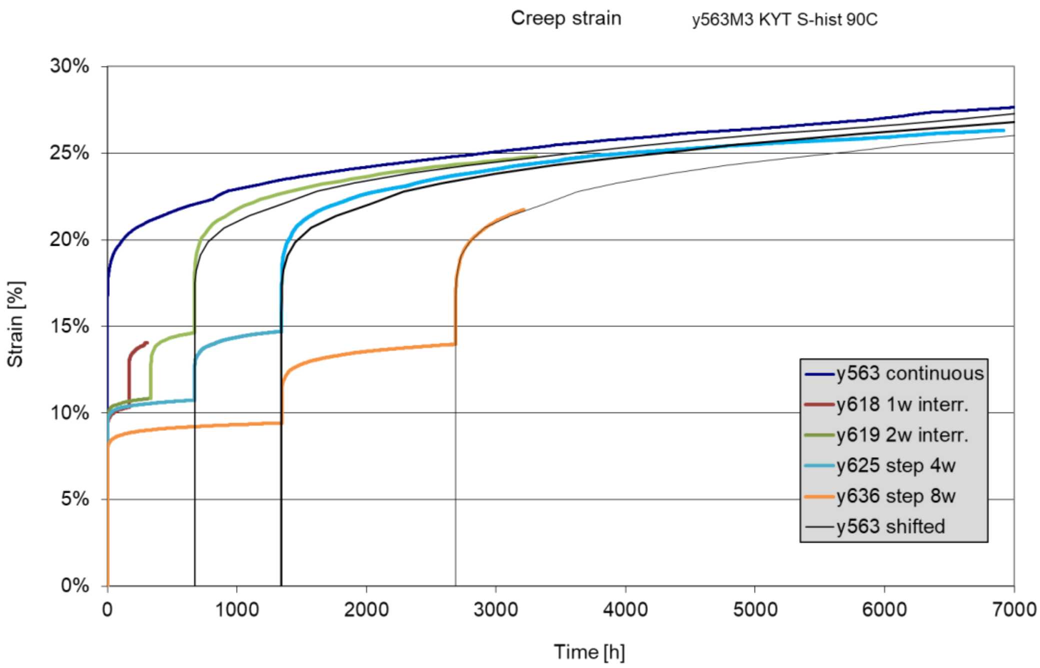

Figure 11. Effect of stepwise loading at 90ºC and 165MPa full load.

This behaviour cannot be predicted by the current creep models and is most likely a result of stabilised dislocation structures collapsing and new dislocations being created when the stress is increased. TEM inspections would be needed to confirm this assumption.

In the repository the swelling pressure and consequently the mechanical stress which the canister experiences, is expected to develop in a monotonous manner, because the geologists say that the hydrostatic pressure will develop steadily without transients. Therefore, although the load history dependence would have been an interesting phenomenon to study, the testing programme was discontinued.

One could argue that if the hydrostatic pressure is applied slowly in the repository, then all creep testing with instant load application is somewhat irrelevant. Instead, maybe the effect of slow constant rate load application on creep rupture strain should be studied. Rupture strain of metals in metals is generally known to decrease as a function of time, so this should be studied for copper as well. This could be realised by a test programme where sample is taken to rupture at a constant strain rate and then the strain rate is decreased, and the effect of decreasing strain rate of rupture strain would be seen.

5. Effect of grain size

The original design of the canister with a pierced & drawn tube with an integrated bottom there were areas in the canister bottom where the grain size was much larger as a result of the forging process and recrystallization. The initial result from SKB [4] indicate that the rupture time of Cu-OFP reduces as the grain size gets larger. Posiva Oy offered to co-fund this theme in the KYT programme and provide suitable test material for creep testing in 2020. However, suitable samples of the bottom with large grain size were not available, so Posiva decided to produce representative grain sizes of 300 to 800 µm by annealing by using a tube batch T83 300 135. Two first heat treatments failed as they produced grain sizes well beyond 1000 µm. The third heat treatment was successful, and the grain sizes of 370, 600 and 800 µm were achieved. The gain size measurements were done by Metlab Oy [6]. Test temperatures of 175ºC and 250ºC were selected because there was some reference data from SKB [5] at different grain sizes at these temperatures.

The creep test results are shown in Table 1. The rupture times compared against the reference data from [5] are shown in Figure 12 at 175ºC and in Figure 13 at 250ºC. In Figure 12 there is a lot of scatter in the reference data, but it is obvious that the rupture time of the KYT series at 175ºC with 370 µm and 600 µm grain sizes differs by orders of magnitude from the reference data. At 250ºC there is about factor of 3 to 6 difference between the KYT results and normal grain size results from batch 500 from [5].

Table 1. Creep test results for the large grain size samples tested at 175ºC and 250ºC.

Code	Ann. Temp.	grain size [µm]	σ (MPa)	T [C]	tr (h)	emin (%/h)	e0 (%)	er (%)	RA (%)	PLM	er/RA	Q	σ/UTS	tr*exp(-Q/RT)
y659M1	725	370	145	175	2.5	3.74E-02	24.5	50	85.1	9143.344	0.587544	1.553	**0.973154**	7.6822E-08
y662M1	725	370	135	175	26.6	2.56E-03	18.4	40.5	76.6	9601.7	0.528721	1.657358	**0.90604**	8.0958E-07
y663M1	725	370	125	175	1060.7	7.98E-05	13.4	35.1	63	10318.91	0.557143	1.424872	**0.838926**	3.2259E-05
y666M4	740	600	125	175	681.0	1.04E-04	14.6	35.8	59.7	10232.66	0.599665	1.264598	**0.848608**	2.0711E-05
y683M2	740	600	120	175	1857.1	4.52E-05	13.0	>34.8	>47.7	10427.93	--	--	**0.814664**	5.6481E-05
y684M19	740	600	130	175	80.8	1.04E-03	17.8	39.4	70.6	9817.903	0.558074	1.497878	**0.882553**	2.45864E-06
y660M10	725	370	100	250	255.3	4.46E-04	9.4	32.8	40.6	11722.23	0.807882	0.643805	**0.769597**	3.0031E-04
y664M10	725	370	90	250	988.2	8.88E-05	7.9	27.4	35	12029.75	0.782857	0.627372	**0.692637**	1.1625E-03
y665M5	740	600	90	250	649.1	1.02E-04	7.8	27	30.1	11934.26	0.89701	0.415815	**0.694444**	7.6360E-04
y682M3	740	600	100	250	169.6	4.09E-04	10.2	26.2	52.6	11629.26	0.498099	1.533634	**0.771605**	1.9946E-04
y685M3	740	600	80	250	2226.3	1.96E-05	5.4	20.9	41.5	12214.29	0.503614	1.400646	**0.617284**	2.6190E-03

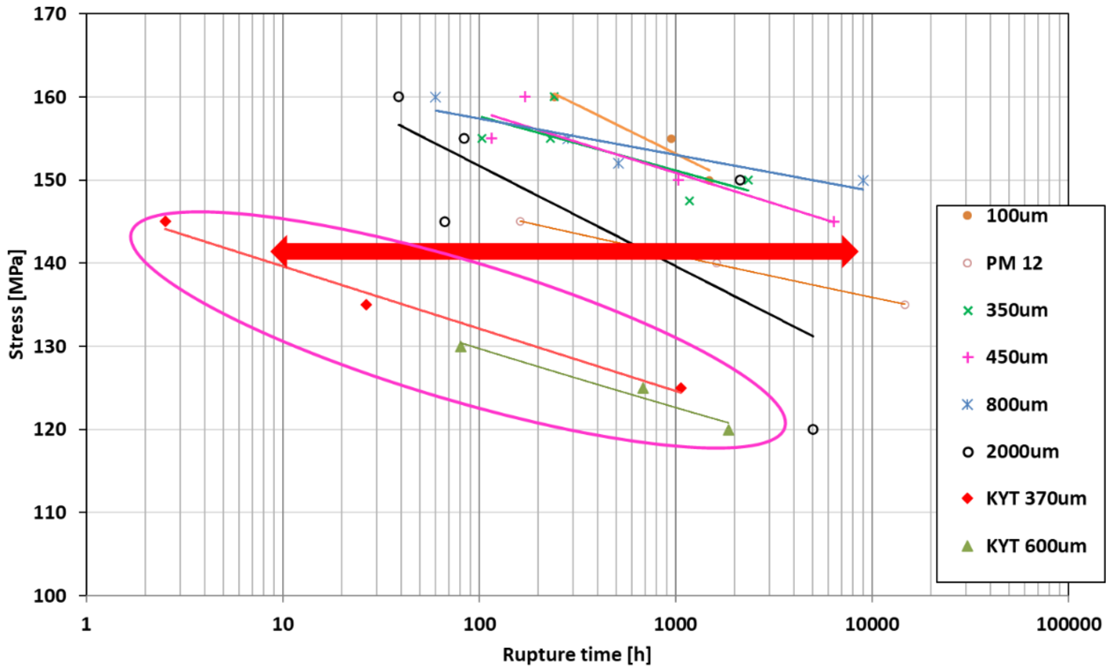

Figure 12. Creep rupture times at 175ºC with grain sizes of 370 µm and 600 µm compared against the reference data from [5].

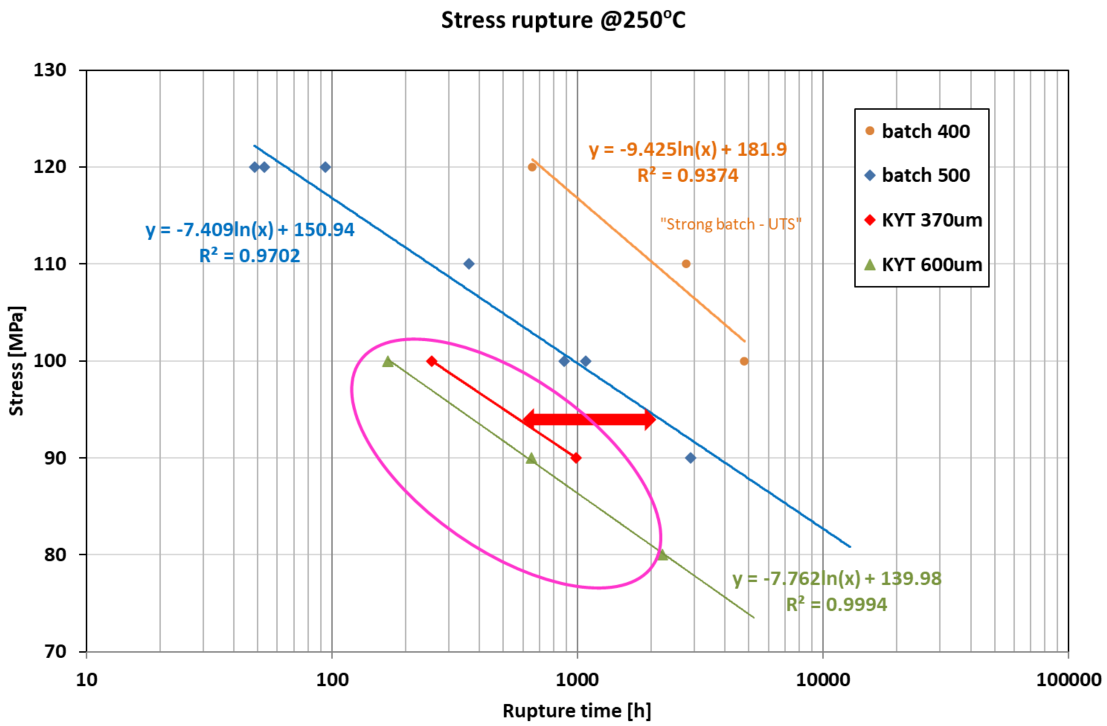

Figure 13. Creep rupture times at 250ºC with grain sizes of 370 µm and 600 µm compared against the reference data from [5].

Although the annealing has produced the wanted grain sizes, it is clear that the rupture times fall short of what would have been expected. This can be the results of the fact that it is not sufficient that a certain grain size is achieved, but also the dislocation density and amount of twinning should be representative. In pure oxygen free (OF) copper there are no other strengthening mechanism which explain the difference. It is assumed that the strengthening mechanism of phosphorus is the same in both cases. In the annealed samples the grain size is achieved by recrystallization and grain growth, which has resulted in a low dislocation density, which is much smaller than in the “normal” copper canister material after the fabrication route which involves heavy deformation and dynamic recrystallization. TEM investigation of the dislocation density would be needed to cast light on the differences, but financial restrictions in the KYT funding have not allowed this to happen.

6. Relaxation

In the repository the canister will experience high hydrostatic pressure accentuated by the swelling pressure of the bentonite. The lid will buckle quickly against the insert and slowly also the cylinder will be pressed against the cast iron insert. The canister will therefore experience a forced displacement loading case where the deformation is limited by the dimensions of the canister, the insert and the air gap between those. In many locations of the canister the deformation stops when the air gap is closed and then the copper will experience a relaxation period at a fixed strain and decreasing stress. At the corner areas the air gap closes more slowly, and the deformation does not stop at all, so in those areas the loading situation is more complex. In the past the copper testing programmes had concentrated mainly on determining the creep properties of copper, but in order to predict the stresses and strains accurately the relaxation behaviour should be also included in the stress analysis by FEM. Therefore, at VTT relaxation testing was introduced into the KYT programme.

In the beginning static relaxation testing was carried out where the test specimen was subjected to a fixed strain and the decreasing stress was monitored during the test period. Kohlrausch relaxation model [8] was used for fitting the data. An example of the fit is shown in Figure 14 where each specimen is loaded to a different strain.

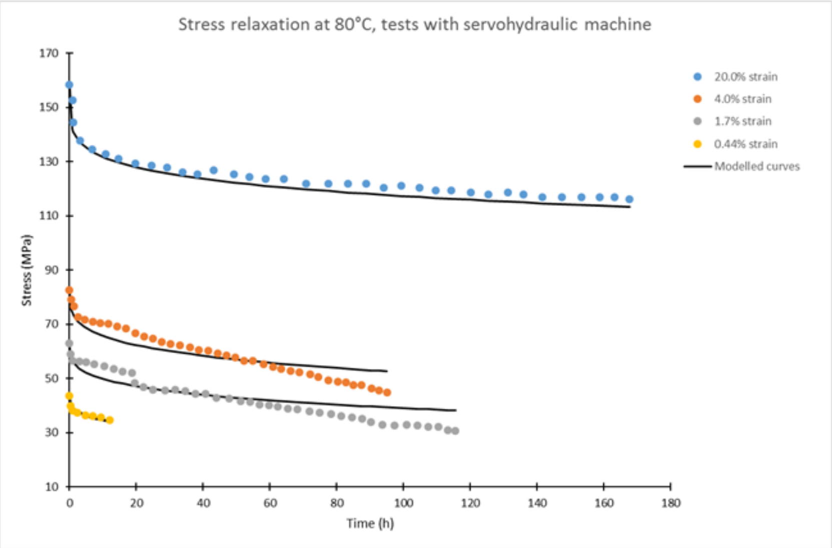

Figure 14. Stress relaxation tests for Cu-OFP at 80°C and the modelled stress relaxation curves.

As next phase cyclic relaxation tests were performed for Cu-OFP. Several stress relaxation periods of 70 to 200 h under tensile stress were applied to test specimens. The strain was decreased to zero and increased back up to the peak strain between these relaxation periods as shown in Figure 15. First, a test with 5 stress relaxation periods was performed at 80°C with 0.6% strain in tension. After that, a test with 3 stress relaxation periods was performed at 80°C with 0.44% strain in tension. Figure 16 shows the stress ratio, i.e. the relaxed stress divided by the peak stress, as a function of time in test at 80°C with 0.6% strain in tension. It can be clearly seen that the amount of relaxed stress decreased as the amount of reloads increased in the test. It can also be seen in Figure 16 that the difference in the peak stresses at the beginning of the stress relaxation periods remained within about 2 MPa in the test. More details of the test programme can be found in [9]. In the new SAFER2028 framework programme the relaxation testing will serve Crystal Plasticity modelling in the MOCRYCO project.

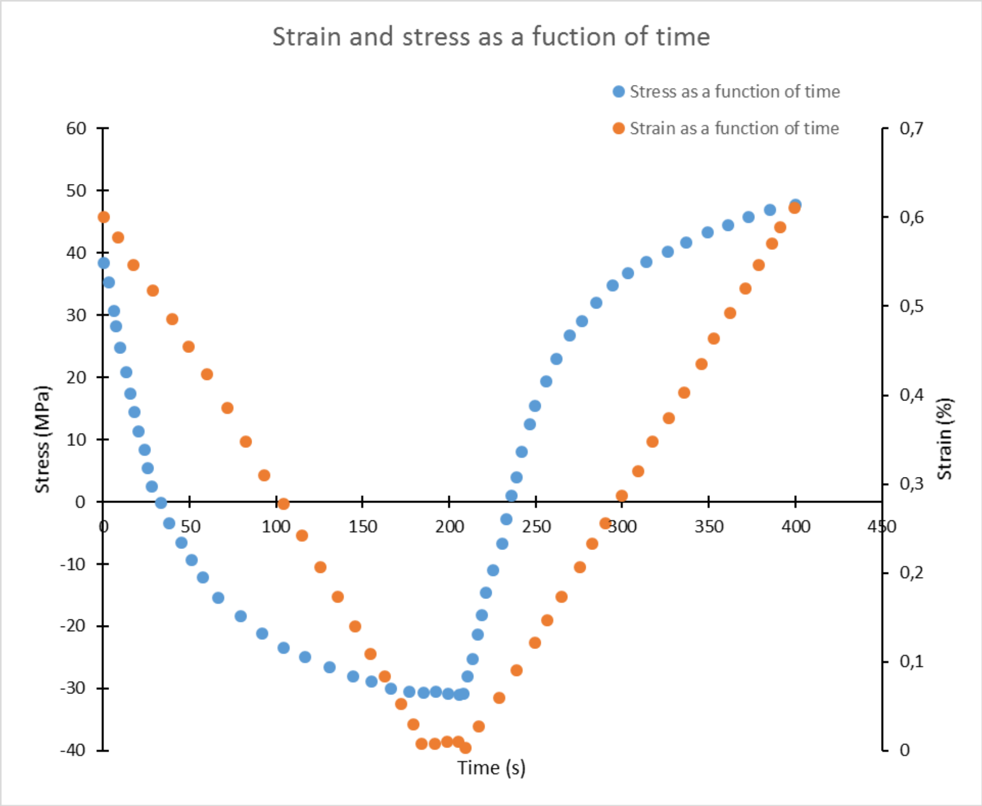

Figure 15. The reload after first (70 h) relaxation period in the cyclic stress relaxation test at 80°C with 0.6% strain in tension

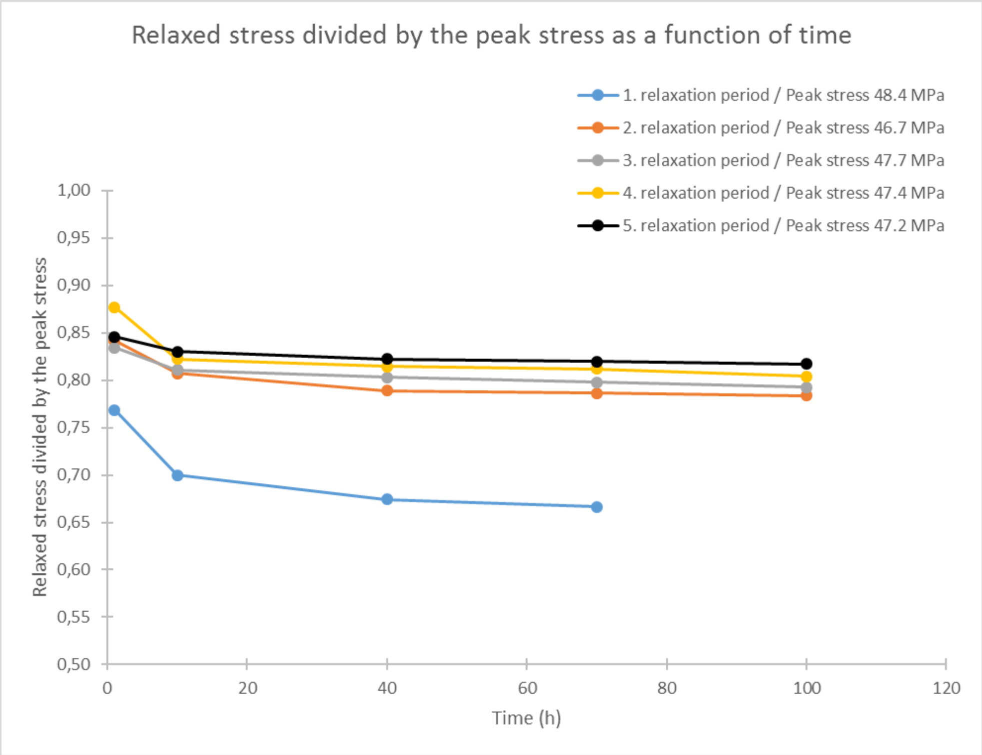

Figure 16. The stress ratio, i.e. the relaxed stress divided by the peak stress, as a function of time in test at 80°C with 0.6% strain in tension

7. Combined effect of creep and corrosion

The plan was to use a Cu-OFP CT-specimen submerged into Olkiluoto reference groundwater at 90ºC and to use wedge loading for maintaining the mechanical stress in the specimen. The purpose of this test was to see if there is a combined effect of creep and corrosion at the tip of the notch of the CT specimen. The notch was wire eroded by 0.25 mm wire allowing free access of the ground water into the notch tip. The CT-specimen was loaded to 35MPa plane stress von Mises reference stress at 90ºC and a copper wedge was pressed to the notch assuming that this would maintain the loading relatively constant during the corrosion test. A small copper vessel and lid were manufactured from Cu-OFP and the vessel was filled with groundwater and placed in a large vessel filled with 90ºC water, circulated by a water pump to maintain the constant temperature. The copper lid was placed on the copper vessel to prevent evaporation of the groundwater. The water temperature was measured only from the surrounding water in order to avoid galvanic corrosion between the CT-specimen and a thermocouple. In this way the CT-specimen was in contact with only the ground water and the copper vessel machined from the same Cu-OFP batch (50mm thick plate).

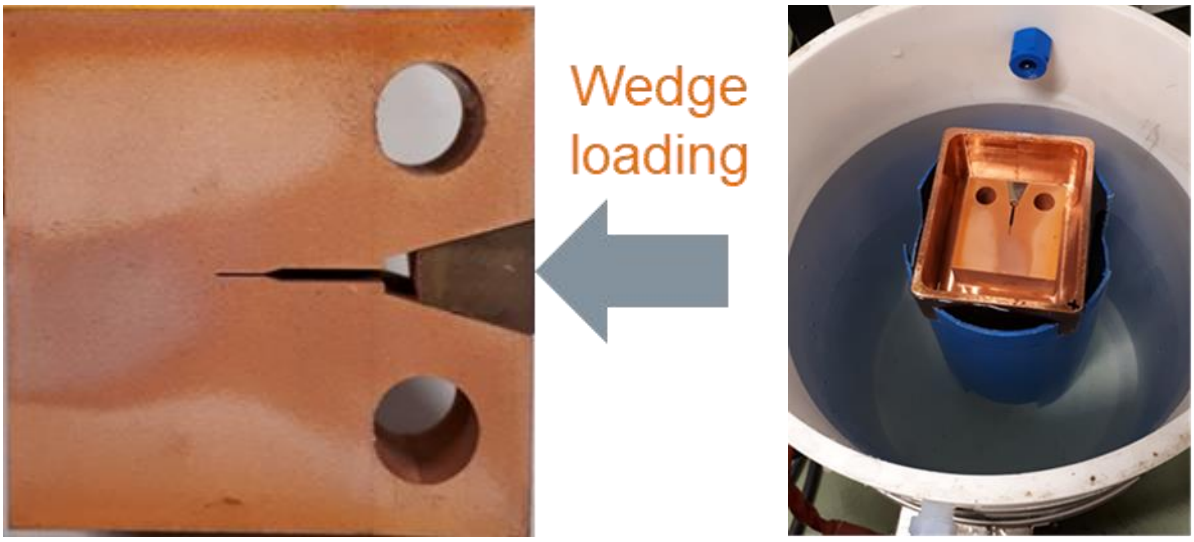

Figure 17. Left: Wire eroded CT specimen (W = 50mm) and Right: the water vessel, small copper vessel and the wedge loaded CT-specimen in place, with the copper lid not yet in place.

Two tests were made with the first test duration of 1000 hours and the second of 5000 hours. After the test the specimen was washed and photographed. The two surfaces of the 5000 hour specimen are seen in Figure 18 showing that there was no crevice corrosion on the bottom surface which had been against the copper vessel during the test. Then the specimen was sectioned, and the tip of the notch was photographed by LOM. The notch tip after the 5000 hour exposure is shown in Figure 19. No combined effect of creep and corrosion is to be seen. By coincidence a grain boundary is located exactly on the centre line of the notch, but no signs of creep cavitation of corrosion at the grain boundary was observed even at a much larger magnification.

It can be argued that possibly the test arrangement was not completely successful in the sense that the wedge loading is not well controlled. It is well possible that the stress level at the notch tip has decreased during the test and possibly already immediately after inserting the wedge, so in that case the chances to observe any combined effects of creep and corrosion might have vanished. This type of testing was then not continued. Other test arrangements might be more effecting for studying the combined effect of creep and corrosion.

Figure 18. Left: bottom surface and Right: top surface of the specimen after the 5000 hour exposure.

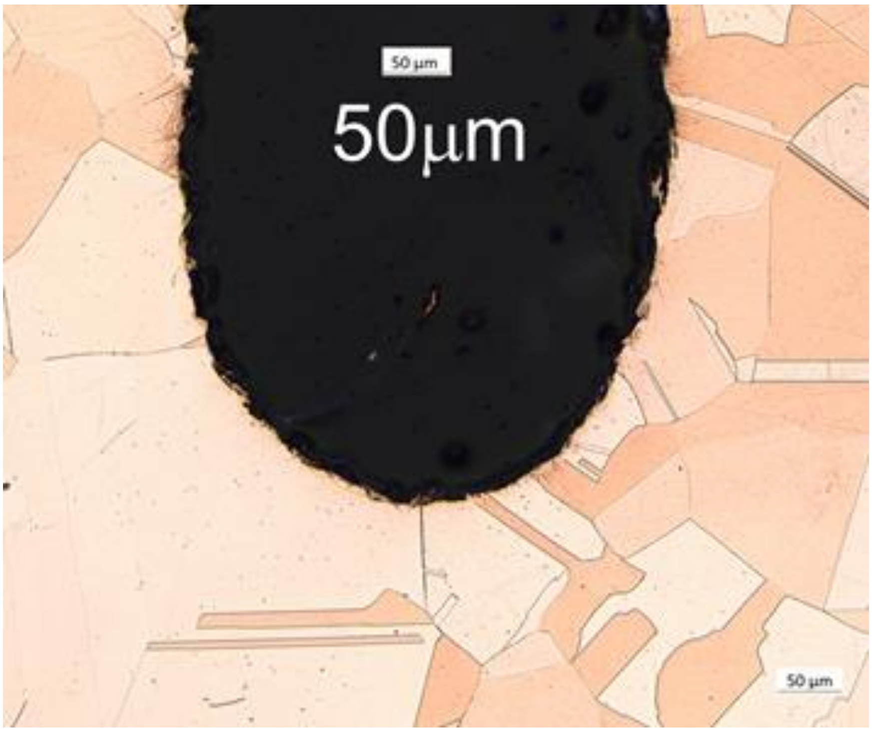

Figure 19. Tip of the notch of the CT specimen after the 5000 hour exposure.

8. Damage behaviour

A M.sc thesis was completed in 2021 [10]. The aim was to assess the cavitation of creep tested, friction stir welded Cu-OFP cross-weld specimens. The cavitation damage was assessed by calculating the cavity density and grain size of the specimens, as well as studying the distribution of the damage throughout the samples. For calculating the cavity density image processing software was used to automate the cavity counting from optical images over a large surface. An open-source image processing software ImageJ was used for the analysis. Different processing tools were tested, and a macro code for ImageJ was written based on the test results. Different sample preparation methods and programs were also tested for use with Cu-OFP. Based on the results, an optimized sample preparation procedure was created. In total, over 2300 LOM images were taken and analysed. The results of the analysis in this thesis show that ImageJ is a viable tool for use in damage assessment due to its efficiency and accuracy.

A series of cross-weld creep tests of friction stir welded copper had previously been done for Posiva Oy and Posiva Oy kindly gave the permission to use these specimens for the thesis work. A typical broken cross-weld test specimen is shown in Figure 20. In all specimens there was more creep cavitation in the weld metal than in the base metal. The grey background colour of the original LOM images was removed to achieve a totally black-and-white image as shown in Figure 21. From the black-and-white image each cavity was identified and numbered for an automated analysis.

The creep cavity number density and area fraction were plotted into images like in Figure 22. Finally, the cavity density and cavity area fraction were plotted against the distance from the fracture surface for visualization like in Figure 23 and Figure 24. The same automated image analysis is now available for analysing other creep tested specimens, either fractured specimens or specimens interrupted at a predefined strain or life fraction.

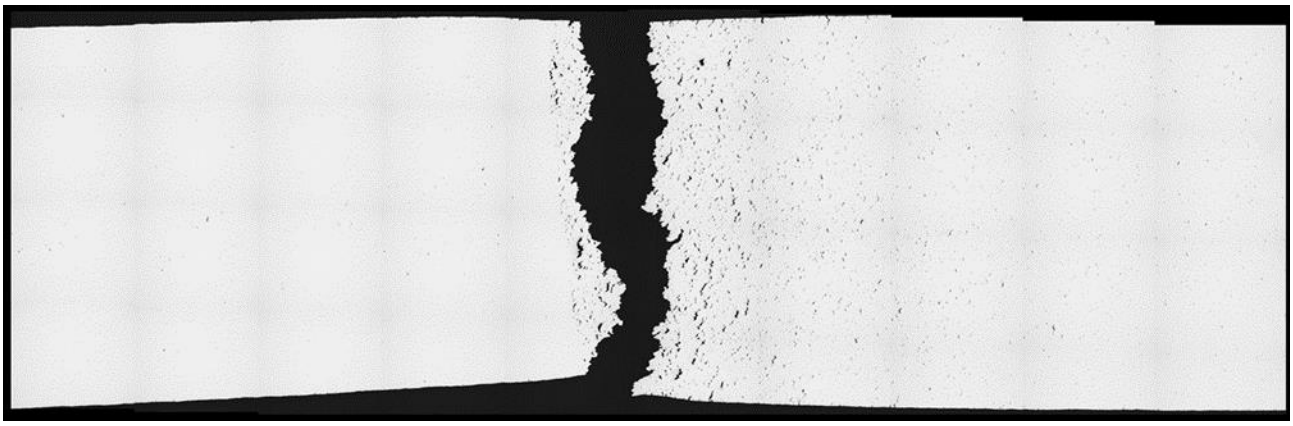

Figure 20. Typical cross-section of a creep tested cross-weld specimen. Cu-OFP base metal on the left and friction stir weld on the right.

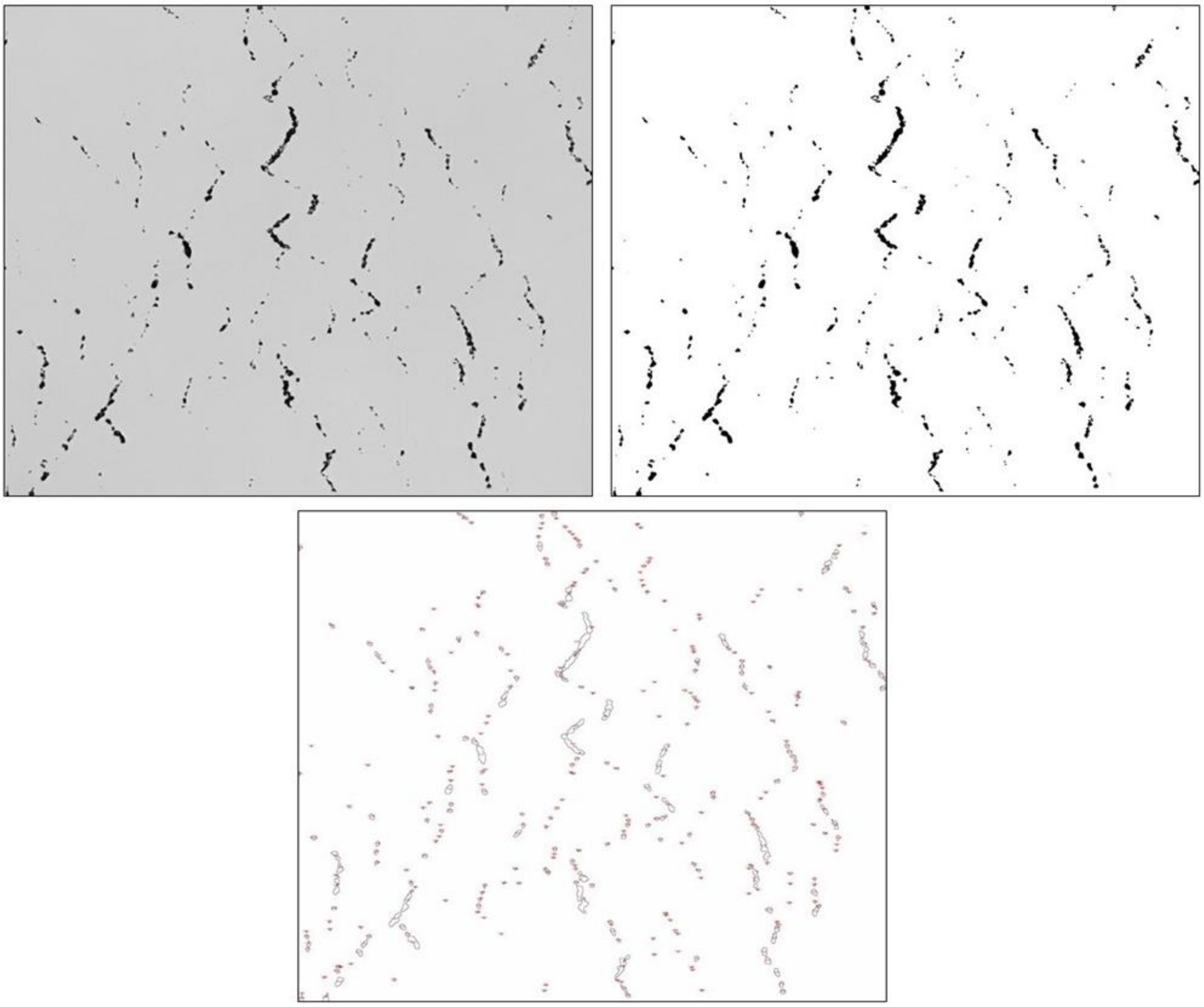

Figure 21. Original LOM image (top left), black-and-white image (top right) and an analyized image with every cavity identified and numbered (bottom).

1	1	7	22	7	4	3	4	6	1	6	4	8	4	7	16	34	24	155	
2	2	1	2	5	3	9	7	2	7	4	7	9	8	23	22	34	28	[illegible]	
3	5	2	8	15	9	4	10	9	9	8	8	9	13	20	25	29	30	194	
4	15	5	5	13	14	10	3	13	16	14	15	14	22	15	12	27	20	194	
5	3	11	8	15	3	4	10	8	17	23	12	15	27	29	13	12	25		
6	4	5	11	18	15	22	7	19	8	15	22	21	15	29	28	29	21		
7	2	9	20	4	7	25	15	14	6	21	22	24	35	37	24	49	38		
8	3	18	10	11	12	29	15	11	15	15	45	18	23	30	26	19	22	138	
9	17	19	9	12	6	19	15	8	22	18	25	13	23	26	28	30	26	82	
10	10	11	5	11	30	9	8	12	16	15	16	10	28	29	28	36	30	141	
11	3	11	8	16	18	14	19	11	24	6	13	22	37	40	31	29	40	131	139
12	7	5	7	5	12	16	13	8	25	18	32	37	35	15	24	30	21	183	
13	8	6	2	8	1	6	4	7	12	13	19	21	38	27	25	24	14	29	
14	3	7	2	5	3	6	7	5	5	12	7	11	10	13	11	8	3		
	19	18	17	16	15	14	13	12	11	10	9	8	7	6	5	4	3	2	1
avg.	5.9	8.4	8.5	10.4	9.8	12.6	9.8	9.5	13.1	13.4	17.6	16.6	22.7	24.3	22.4	27.9	24.4	145.0	139.0
den.	16	23	23	29	27	35	27	26	36	37	49	46	63	67	62	77	67	400	384

220	289	352	336	300	396	383	451	403	479	378	427	463	410	357	531	535	461	454	1
296	266	376	374	386	423	355	454	338	400	526	450	428	491	502	527	592	369	393	2
170	388	442	420	410	387	322	400	432	524	522	411	456	439	447	444	594	475	507	3
217	368	543	585	384	391	416	482	444	419	392	332	543	478	422	470	512	420	544	4
295	591	675	445	449	453	407	414	338	439	371	417	439	412	408	522	482	467	508	5
269	696	675	591	615	500	412	410	458	452	420	416	406	392	444	420	321	444	358	6
340	548	474	549	608	520	567	430	360	429	430	336	440	448	458	498	383	370	403	7
	435	586	516	494	440	418	489	429	422	441	479	451	431	441	464	398	443	519	8
	336	617	583	458	472	458	652	390	424	452	391	431	400	414	423	383	393	471	9
	346	714	601	402	513	498	448	392	404	367	454	472	430	349	389	403	343	386	10
	343	438	591	501	477	430	335	409	392	473	508	408	426	506	367	356	358	382	11
169	293	494	468	445	542	337	406	371	396	412	378	321	359	358	432	442	353	408	12
219	266	430	333	345	428	413	425	404	417	448	400	377	377	331	345	403	263	380	13
162	256	213	304	332	378	338	338	379	432	410	394	442	343	346	383	357	349	356	14
1	2	3	4	5	6	7	8	9	10	11	12	13	14	15	16	17	18	19	
235.7	387.2	502.1	478.3	437.8	451.4	411.0	438.1	396.2	430.6	431.6	413.8	434.1	416.9	413.1	443.9	440.1	393.4	433.5	avg.
878	1097	1404	1344	1209	1246	1135	1210	1094	1189	1192	1143	1199	1151	1141	1226	1215	1086	1197	den.

Figure 22. Cavity density grid with a cavity number count in each cell and cells coloured to highlight areas of high cavity density. weld metal on the right.

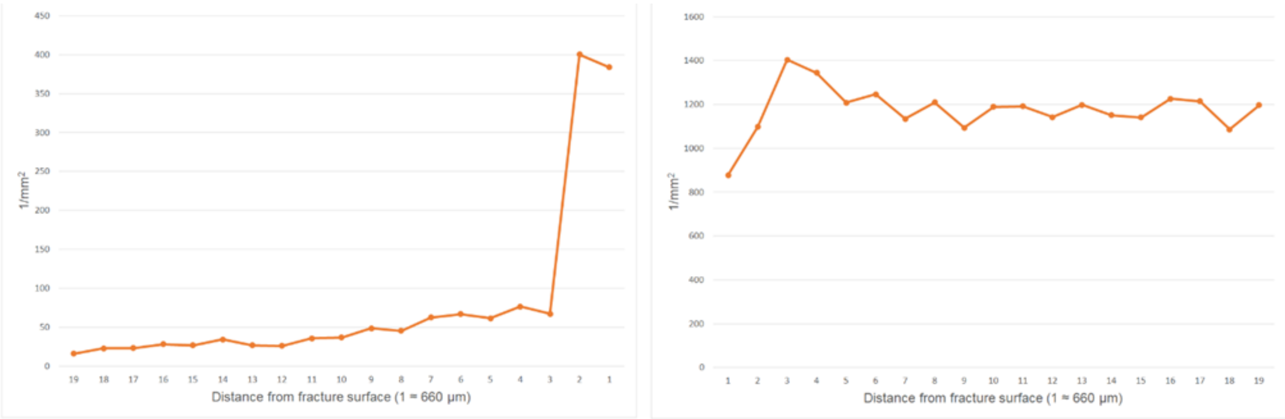

Figure 23. The cavity density vs. distance from the fracture surface, data from Figure 22.

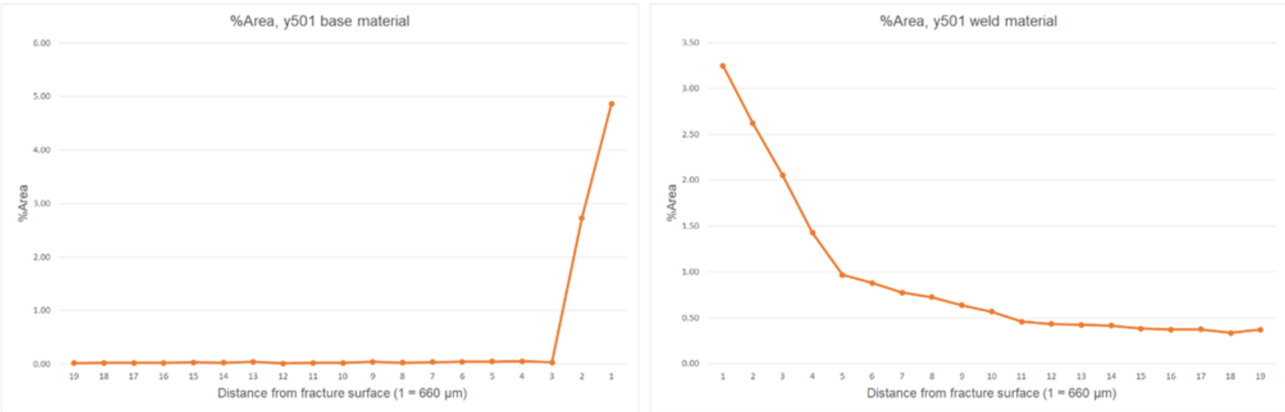

Figure 24. Area density of cavities from Figure 22 vs. distance from the fracture surface.

Furthermore, more detailed studies on the creep cavitation damage were conducted by investigating the size and shape of creep cavities using scanning electron microscope. Figure 25a shows a faceted creep cavity in grain boundary and Figure 25b presents a triangular cavity in a triple junction.

a) b)

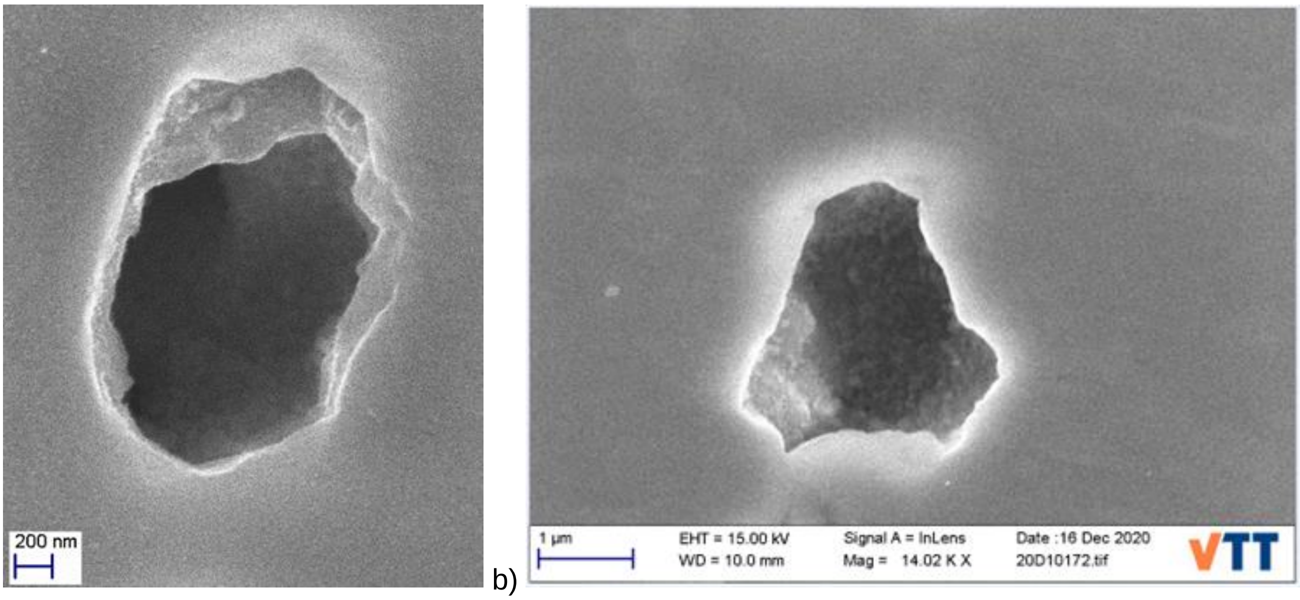

Figure 25. A *faceted creep cavity in grain boundary in a), a triangular cavity in a triple junction in b).*

Based on e.g. copper material creep cavitation studies (along with selected steel materials), a new material damage model based on the creep cavitation propagation was developed during the course of the project and published in a scientific journal [11]. It is widely acknowledged that remaining life of material/component is proportional to the creep cavitation measure, such as cavitation area fraction. A classical creep cavitation model suggests the cavitation damage area fraction to be dependent on the strain, time, stress and temperature that the material/component has experienced so that;

$$\Phi' = A'\varepsilon t\sigma^{n'}e^{-Q/RT} \quad (1)$$

where *A'* is material dependent parameter, *σ* is stress, *n´* is stress exponent, *Q* is the apparent activation energy, close to that for grain boundary diffusion, *R* is the gas constant, and *T* is absolute temperature. The advantage of the new model stems from avoiding measured creep strain that can be inaccessible in many practical structures, and cavitation damage area fraction can be modelled based on time, stress and temperature so that;

$$\Phi = B(T,\sigma)t(t/t_{ref})^{1+m}(\sigma/G)^{n+\omega}e^{-Q/RT} \quad (2)$$

where m and ω are material parameters covering microstructural damage and e.g. stress increase in the case of constant load testing, B emerges from power-law creep equation and G is shear modulus.

References

1. Kansallinen ydinjätehuollon tutkimusohjelma KYT2022. Puiteohjelma tutkimuskaudelle 2019 - 2022.
2. Raiko, H. Canister Design 2012. Report POSIVA 2012-13, Posiva Oy.
3. Wilshire, B. & Bache, M. B. Cost effective prediction of creep design data for power plant steels. 2nd Intl. ECCC Conference on Creep & Fracture in High Temperature Components – Design & Life Assessment. April 21-23, 2009, Dübendorf, Switzerland.
4. K. Mannesson, H. C. M. Andersson-Östling, Stress application and the effect on creep of copper, May 2016, SKB R-14-31
5. H. C. M. Andersson-Östling, R. Sandström, Survey of creep properties of copper intended for nuclear waste disposal, Dec. 2009, SKB R-09-32
6. T. Karhula, Test Report No. 212988, METLAB Oy, 8.12.2021
7. Holmström, S. Engineering tools for robust creep modeling. Dissertation. Espoo, VTT, 2010. VTT Publications 728. 94 p. + app. 53 p.
8. P. Auerkari, R. Pohja, A. Nurmela, Relaxation of OFP copper, VTT Research Report, VTT-R-00366-14.
9. R. Pohja, A. Nurmela, Stress relaxation assessment to support the crystal plasticity model for copper, VTT-R-01088-19
10. J. Vihko, Damage Assessment of Friction Stir Welded Copper Cross-weld Specimens, M.Sc thesis, Aalto Univ., 7/2021
11. R. Pohja, P. Auerkari, P. Vilaça, Modelling for creep cavitation damage and life of three metallic materials, Materials at High Temperatures 39(1) (2022) 86-96, https://doi.org/10.1080/09603409.2021.2024420